Journal of Solid State Chemistry **160,** 307–310 (2001)
doi:10.1006/jssc.2001.9211, available online at http://www.idealibrary.com on IDEAL®

Pressure Dependence of the Lattice Distortion in Perovskite $La_{0.5-x}Bi_xCa_{0.5}MnO_3$ ($x = 0.1, 0.15, 0.2$)

X. Wang,[1] Y. W. Pan, Q. L. Cui, J. Zhang, W. Gao, and G. T. Zou

National Laboratory for Superhard Materials, Jilin University, Changchun 130023, People's Republic of China
E-mail: aliacxin@netease.com

Received December 21, 2000; in revised form April 4, 2001; accepted April 12, 2001

The *in situ* behavior of distorted perovskite $La_{0.5-x}Bi_xCa_{0.5}MnO_3$ ($x = 0.1, 0.15, 0.2$) under high pressure has been studied by energy-dispersive X-ray diffraction in a diamond anvil cell. An abnormal change of the 202–040 *d*-spacing ascribed to the disappearance of the distortion mode Q_2 in the MnO_6 octahedra is observed at 1.2, 1.4, and 1.6 GPa, respectively, and it results in a reduction of the Jahn–Teller distortion commonly existing in the manganites. Effect of the unique $6s^2$ long-pair character of the Bi^{3+} ion on the pressure dependence of the lattice distortion is discussed. © 2001 Academic Press

Key Words: **energy-dispersive X-ray diffraction; Jahn–Teller distortion; $La_{0.5-x}Bi_xCa_{0.5}MnO_3$; manganites; perovskite; pressure.**

INTRODUCTION

In the perovskite $RE_{1-x}A_xMnO_3$ (RE = rare earth ions, A = alkaline earth ions) compounds, the magnetic cation–anion–cation exchange interactions and electronic structures have exhibited very intriguing fundamental physical phenomena reported several decades ago (1, 2). Recent attention has been given to an unexpectedly rich variety of behaviors originating in the strong coupling between the electronic, magnetic, and structural degrees of freedom, and these are observed characteristically in the system $La_{1-x}Ca_xMnO_3$ (3–7). As a function of temperature and doping, this system displays various phase transitions. In the range $0.2 < x < 0.45$ the system is a ferromagnetic metal at low temperatures, displaying colossal magnetoresistance (CMR) effects near T_C. As x approaches 0.5, a transition from a paramagnetic to a ferromagnetic state is followed by an antiferromagnetic charge-ordered state upon lowering the temperature. For the larger hole-density regime, no detailed investigation has been carried out for $La_{1-x}Ca_xMnO_3$. On the other hand, a study of $Bi_{1-x}Ca_xMnO_3$ has been investigated by Bokov *et al.* (8). Since the ionic radii of trivalent bismuth and trivalent lanthanum are very close to each other ($Bi^{3+} \sim 1.24$ Å, $La^{3+} \sim 1.22$ Å, in nine-coordination), one may expect similar physical properties between them. Interestingly, however, a long-range order of charges was only reported in the Mn^{4+}-rich regime of $Bi_{1-x}Ca_xMnO_3$ and no evidence for metallicity was found for a wide range from $x = 0.3$ to $x = 0.9$ for $H = 0$ (8, 9). In the $x = 0$ endmember of the solid solution, $LaMnO_3$ shows the A-type antiferromagnetism with an orthorhombic $GdFeO_3$-type structure, while $BiMnO_3$ exhibits ferromagnetism with a triclinically distorted perovskite structure. These discrepancies may come from the high-polarizability $6s^2$ long pair of the Bi^{3+} ion (10, 11). So the need to investigate the effects of the bismuth cation on the physical properties of these mixed-valent manganites is necessary, and structural studies will be of value for a better understanding of the systems. In this paper, we have carried out in situ X-ray diffraction studies on $La_{0.5-x}Bi_xCa_{0.5}MnO_3$ ($x = 0.1, 0.15, 0.2$) under high pressure with synchrotron radiation. By application of hydrostatic pressure, an abnormal change of the 202-040 *d*-spacing was found in all the samples. With the concentration x increasing, the turning pressure for this change also increases, and the effect coming from the $6s^2$ long-pair character of the Bi^{3+} ion is discussed.

EXPERIMENTAL

The polycrystalline samples $La_{0.5-x}Bi_xCa_{0.5}MnO_3$ ($x = 0.1, 0.15, 0.2$) were synthesized by a standard ceramic technique. Appropriate starting materials of La_2O_3, Bi_2O_3, $CaCO_3$, and MnO_2 were mixed and ground for about an hour, and then calcined at 700°C for 24 h in air. After this, the powders were milled and reacted again. The resulting powder was pressed into pellets, and sintered at 1100°C in air for 48 h. Finally, the specimens were slowly cooled down in air over a period of 12 h. Powder X-ray diffraction data of the prepared samples were collected using a REGAKU diffractometer with monochromated Cu$K\alpha$ radiation by

[1] To whom correspondence should be addressed. Fax: 86-0431-8920398.

0022-4596/01 $35.00

step scanning (0.02°) in the range $20° \leq 2\theta \leq 100°$, and all were found to be single phase. The unit cell dimensions were determined from observed d-spacings by the least-squares method.

All the high-pressure X-ray diffraction patterns employing an energy-dispersive method were recorded on the wiggler beamline (3W1A) of the Beijing Synchrotron Radiation Laboratory (BSRL). A diamond cell with type-I diamonds brilliant cut with 350-μm culets was driven by an accurately adjustable gear-worm-level system. The relation between the peak energy E_{hkl} and the channels in the multichannel analyzer (MCA) was calibrated using the fluorescence peaks of Sn, Pt, Cs, and Br. The powder samples were loaded into the 140-μm diameter chamber of a stainless steel gasket with very fine Platinum or with Aurum powder, which was served as the inner pressure calibrant. A mixture of methanol/ethanol 4:1 was used as the pressure medium. Pressure was determined from the (111) and (200) peaks of Au or Pt along with its respective equation of state. The polychromatic X-ray beam was collimated to a $60 \times 60\ \mu m^2$ sized spot with the storage ring operating at 2.8 GeV and 90–50 mA. The diffraction 2θ angle between the direct beam and the detector was set at $\sim 17°$.

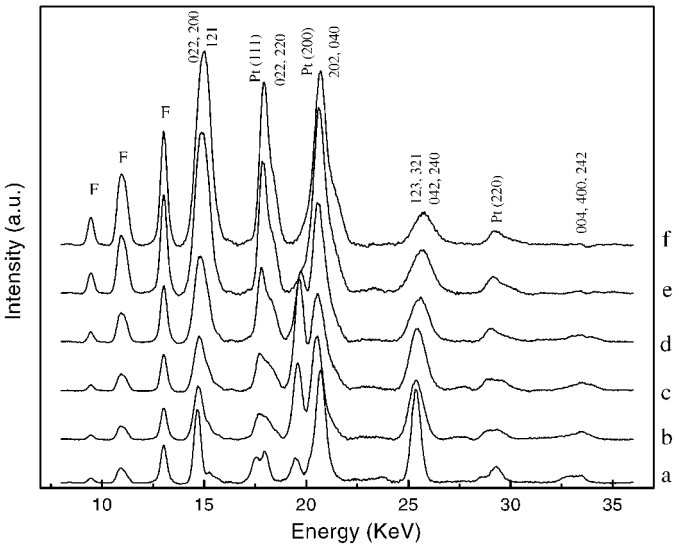

FIG. 1. Energy-dispersive X-ray diffraction patterns of $La_{0.4}Bi_{0.1}Ca_{0.5}MnO_3$ as a function of pressure. Remarkable change appears in the spectra at about 21 keV. The pressure for spectra (a) to (f) is at 0, 1.4, 6.8, 11.6, 15.6, and 19.9 GPa, respectively. F—fluorescence peak.

RESULTS AND DISCUSSION

From powder X-ray diffraction patterns at ambient pressure, the crystalline products are pure phase and the orthorhombic unit cell is adopted for all the samples investigated because of only a small shift of the diffraction peaks. A small expansion of the molar volume with bismuth substitution is found and coincides with the fact that the ionic radius of Bi^{3+} is slightly larger than that of La^{3+}.

Three separate runs for $x = 0.1$, 0.15, and 0.2 are carried out up to 19.9, 14.8, and 45.8 GPa, respectively. In the energy-dispersive runs, not all diffraction peaks in powder X-ray diffraction for three compositions can be included but only four main peaks are chosen to be examined because of the narrow energy range (between 3 and 40 keV). The energy-dispersive X-ray diffraction patterns for $x = 0.1$ at selected pressures are shown in Fig. 1. As can be seen, at the beginning of the spectrum, there are fluorescence peaks coming from La, Bi, and Pt. The peak positions in the spectrum can be distinguished by the method of fitting multipeaks. Higher pressure leads to a decrease in the intensities of peaks and a general degradation of the peak-to-background ratio in the diffraction pattern. This is related to the strength of the materials. The broadening of the peaks may be caused by the deviatoric stress in the sample chamber under high pressure.

According to the energy dispersion equation $E \cdot d = (0.619927/\sin\theta)$(keV.nm), the corresponding d-spacings as a function of pressure for $La_{0.5-x}Bi_xCa_{0.5}MnO_3$ ($x = 0.1$, 0.15, 0.2) are shown in Fig. 2. As can be seen from the figure, most d-spacings behave normally as they all decrease smoothly with increasing pressure. However, it is unusual for the 202–040 d-spacing as shown in Fig. 3, which expands upon compression from the beginning, and then contracts when further pressurized above certain pressure. This phenomenon is quite reproducible and the turning pressure for all three compositions is at 1.2, 1.4, and 1.6 GPa, respectively. At room temperature, both energy-dispersive and powder X-ray diffractions observe a single peak that is a combination of the unresolved (202) and (040) nuclear structure peaks. Although the relative contribution from the (202) and (040) reflections to this unusual change is not clear, we suppose that it is mainly from the (202) reflection. Radaelli and coworkers have reported that an increase of the (202) d-spacing and an unusual broadening of the 202–040 diffraction peaks of $La_{0.5}Ca_{0.5}MnO_3$ with lowering the temperatures are found in their high-resolution synchrotron X-ray patterns (6, 7). In the present work, we have not been able to determine positional parameters and we have no direct evidence of the cation distribution. However, some qualitative estimates can be derived from the results of Radaelli *et al.* This abnormal change of the 202–040 d-spacing is intimately related to the structural characteristics of the ABO_3 compounds, especially for manganites. One of the key factors in these oxides is the Jahn–Teller distortions due to the Mn^{3+} ions, which have the $3d^4: t_{g2}^3 e_g^1$ electron configuration, and these severely deformed oxygen octahedra exhibit more prominently in the endmember $LaMnO_3$ (12, 13). Generally, the Jahn–Teller distortion can be described by the combination of an apically compressed type Q_2, and an apically elongated type

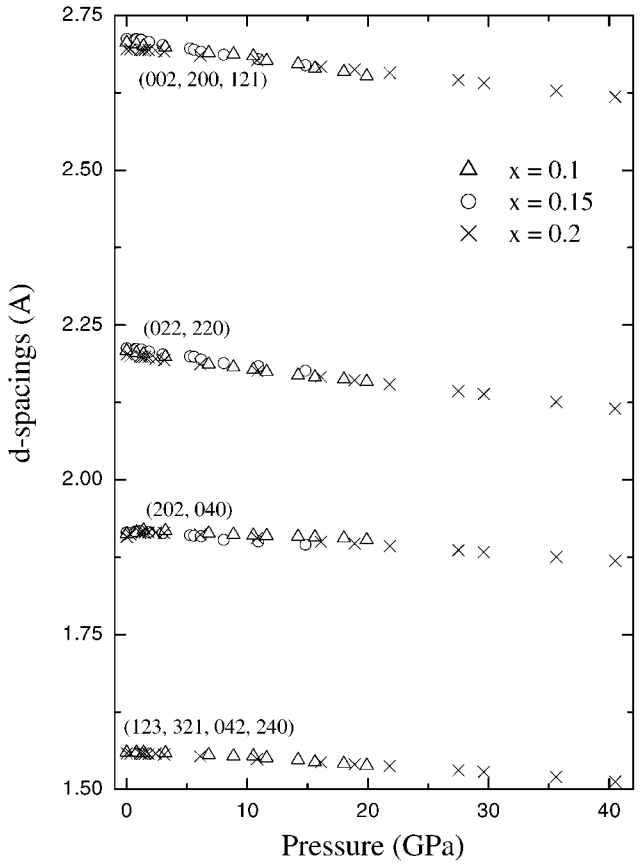

FIG. 2. The effect of pressure on the *d*-spacings of $La_{0.5-x}Bi_xCa_{0.5}MnO_3$ ($x = 0.1, 0.15, 0.2$). For clarity, fluorescence lines are not plotted in the figure.

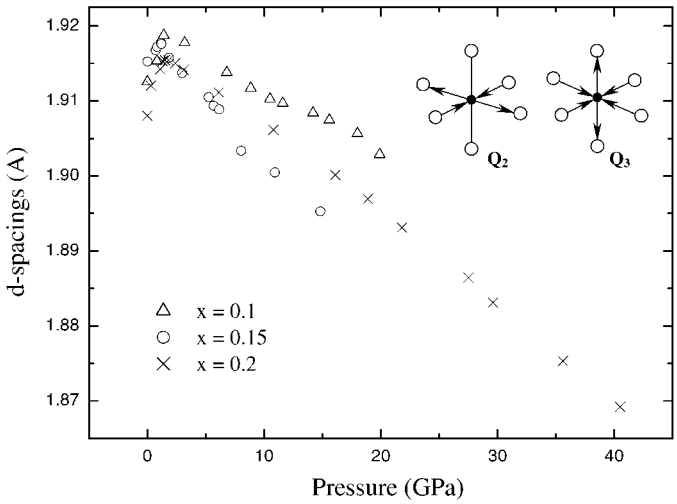

FIG. 3. The effect of pressure on the 202–040 *d*-spacings of $La_{0.5-x}Bi_xCa_{0.5}MnO_3$ ($x = 0.1, 0.15, 0.2$). The turning pressure is at 1.2, 1.4, and 1.6 GPa, respectively. In the inset, the basal-plane distortion mode Q_2 and the octahedral stretching mode Q_3 are shown.

Q_3 in the basal plane of the MnO_6 octahedra and these two kinds of distortions are shown in the inset of Fig. 3. The appearance of the change in Fig. 3 could be associated with the displacement of the cations and coordination oxygen atoms under high pressure. In a simple view, the 202–040 reflections can reflect the variations of the *a*–*c* plane and the *b* axis in the deformed MnO_6 octahedra directly. The application of hydrostatic pressure will drive the oxygens in the basal-plane diagonals closer to the center of the MnO_4 square, and favor the displacement of the basal-plane oxygen atoms contracting and the apical oxygen atoms extending from their ideal positions. As a consequence, in this particular instance, diffraction is much more sensitive to this distortion. When pressure increases up to a certain point, the basal-plane distortion Q_2 progressively vanishes and the results are reflected in the special change of the 202–040 *d*-spacing. A similar disappearance of the Q_2-type basal-plane distortion has been observed in isostructural $La_{0.65}Y_{0.05}Ca_{0.3}MnO_3$ perovskite, accompanying the insulator-to-metal transition with lowering the temperature (14). However, despite the similarity that the dropout of the Q_2-type distortion can be thermally driven or pressure-induced, the effect of pressure is more effective than that of temperature on the lattice distortions. Application of hydrostatic pressure can directly affect the atom positions and determine the degree of close-packing of cations, while the interactions among charge, orbital, and spin coupling to the lattice structure can be enhanced through a hysteresis process with lowering temperatures.

As we can see from the Fig. 3, with doping concentration *x* increasing, the pressure needed for the turning point also increases. This effect can be ascribed to the $6s^2$ long-pair character of the Bi^{3+} ion. When the long-pair character is dominant, the bismuth cation in the crystal would shift from the center of the hexagon of the oxide anion and have a tendency to result in a lowering of the symmetry of the local structure. But when the Bi^{3+} ion is forced into high symmetry, it would release such distortions, and the long-pair character becomes constrained (15, 16). As discussed above, under high pressure, all atom distances are compressed and the disappearance of the basal-plane distortion mode of Q_2 will give more perfect octahedra with the MnO_4 equatorial square planes, while it is accompanied with the change of the $6s^2$ long-pair character of the Bi^{3+} ion. With doping more Bi^{3+} ions, it needs higher pressure to overcome the extra elastic-energy cost of the deformations, and therefore raises the turning pressure above which the character becomes constrained.

In conclusion, an *in situ* X-ray diffraction study on the pressure dependence of the lattice distortion in $La_{0.5-x}Bi_xCa_{0.5}MnO_3$ ($x = 0.1, 0.15, 0.2$) was performed using synchrotron radiation. With increasing pressure, an

abnormal change of the 202–040 *d*-spacing due to the amiable coupling among the charge, spin, and orbitals in the whole structure was observed and suggested the disappearance of the octahedral stretching mode Q_2 within the *a*–*c* basal plane of the MnO_6 octahedra. The turning pressure for this change also shows the dependence of the concentration *x*, and induces the $6s^2$ long-pair character of the bismuth cation to change from the dominant one to the constrained one.

ACKNOWLEDGMENTS

This work was supported by the Basic Research Project of the Ministry of Science and Technology of China, the National Doctoral Foundation of the China Education Commission under Grant 89018316 and partially supported by the National Natural Science Foundation of China.

REFERENCES

1. G. H. Jonker and J. H. Van Santen, *Physica* **16,** 337 (1950).
2. E. O. Wollan and W. C. Koehler, *Phys. Rev.* **100,** 545 (1955).
3. S. Jin, T. H. Tiefel, M. McCormack, R. Fastnacht, R. Ramesh, and L. H. Chen, *Science* **264,** 413 (1994).
4. P. E. Schiffer, A. P. Ramirez, W. Bao, and S.-W. Cheong, *Phys. Rev. Lett.* **75,** 3336 (1995).
5. C. H. Chen and S.-W. Cheong, *Phys. Rev. Lett.* **76,** 4042 (1996).
6. P. G. Radaelli, P. E. Cox, M. Marezio, S.-W. Cheong, P. E. Schiffer, and A. P. Ramirez, *Phys. Rev. Lett.* **75,** 4488 (1995).
7. P. G. Radaelli, P. E. Cox, M. Marezio, and S.-W. Cheong, *Phys. Rev. B* **55,** 3015 (1997).
8. V. A. Bokov, N. A. Grigoryan, and M. F. Bryzhina, *Phys. Status Solidi* **20,** 745 (1967).
9. H. Chiba, M. Kikuchi, Y. Muraoka, and Y. Syono, *Solid State Commun.* **99,** 499 (1996).
10. J. B. A. A. Elemans, B. Van-Laar, K. R. Van Der Veen, and B. O. Loopstra, *J. Solid State Chem.* **3,** 238 (1971).
11. H. Chiba, T. Atou, and Y. Syono, *J. Solid State Chem.* **132,** 139 (1997).
12. J. B. Goodenough, *Phys. Rev.* **100,** 564 (1955).
13. P. Norby, I. G. Krogh Andersen, and E. Krogh Andersen, *J. Solid State Chem.* **119,** 191 (1995).
14. J. L. García-Müoz, M. Suaaidi, J. Fontcuberta, J. Rodríguez-Carvajal, *Phys. Rev. B* **55,** 34 (1997).
15. A. W. Sleight and G. Jones, *Acta Crystallogr. Sect. B* **31,** 2748 (1975).
16. T. Atou, H. Chiba, K. Ohoyama, Y. Yamaguchi, and Y. Syono, *J. Solid State Chem.* **145,** 639 (1999).